Experimental study of vortex shedding mitigation in circular cylinders with helical strakes

Estudo experimental sobre a mitigação da libertação de vórtices em cilindros circulares com alhetas helicoidais

Lucas Lopes[1] | Luís Eça [1] | Fernando Marques da Silva [2] | Fernando Oliveira [2]

[1] Instituto Superior Técnico, Universidade de Lisboa; lucas.lopes@tecnico.ulisboa.pt, luis.eça@tecnico.ulisboa.pt

[2] Laboratório Nacional de Engenharia Civil (LNEC); jaiselmeer@gmail.com, fvoliveira@lnec.pt

https://doi.org/10.82452/me20263705

abstract

An experimental investigation of vortex shedding mitigation in circular cylinders using helical strakes with a controlled gap from the surface was carried out. While conventional attached strakes effectively suppress vortex-induced vibrations (VIV), they introduce significant drag penalties. The spaced-strake concept aims to maintain wake decoherence while reducing this aerodynamic cost. Wind tunnel experiments were conducted on a smooth baseline cylinder and three configurations with gaps relative to the cylinder surface of 20%, 40%, and 60% of the strake height. Aerodynamic forces and surface pressures were measured to assess wake behavior. Results show that spaced strakes significantly reduce lift fluctuations while decreasing drag penalties as the gap increases. Pressure data indicate enhanced momentum exchange and partial base-pressure recovery, especially for the largest gap. Overall, spaced helical strakes offer an effective compromise between drag reduction and VIV suppression.

Keywords: Vortex-shedding, Helical strakes, Drag reduction, Vortice-induced vibrations, Wind tunnel

resumo

Uma investigação experimental relativa à mitigação do desprendimento de vórtices em cilindros circulares utilizando alhetas helicoidais com um afastamento controlado da superfície foi feito. Embora as alhetas convencionais, fixas à superfície, sejam eficazes na supressão de vibrações induzidas por vórtices (VIV), introduzem penalizações significativas na resistência aerodinâmica. O conceito de alhetas espaçadas visa promover a quebra de coerência da esteira, reduzindo esse custo aerodinâmico. Os ensaios foram realizados em túnel de vento de baixa turbulência, com um cilindro de referência liso e três configurações com afastamentos relativos à superfície de 20%, 40% e 60% da altura da alheta. Foram medidas forças aerodinâmicas e distribuições de pressão superficial para analisar o comportamento da esteira. Os resultados mostram que a configuração espaçada reduz significativamente as flutuações de sustentação e diminui a penalização de resistência à medida que o afastamento aumenta. As medições de pressão indicam maior troca de quantidade de movimento e recuperação parcial da pressão de base, sobretudo para o maior afastamento. Globalmente, as alhetas helicoidais espaçadas constituem um compromisso eficaz entre redução de resistência aerodinâmica e supressão de VIV.

Palavras-chave: Libertação de vórtices, Alhetas helicoidais, Redução da resistência, Vibrações induzidas por vórtices, Túnel de vento

1- INTRODUCTION

Cylindrical components are widely used in engineering structures and often experience unsteady aerodynamic loads when exposed to crossflow. Helical strakes are a well-established passive control solution for suppressing VIV by disrupting the spanwise coherence of the wake [1]. However, their conventional attached configuration typically induces a substantial drag penalty, reducing overall aerodynamic efficiency. This work proposes and investigates an alternative concept in which the helical strakes are spaced from the cylinder surface, introducing a finite gap intended to decrease drag penalties while maintaining vortex shedding coherence disruption. To assess this idea, an experimental campaign was conducted in a low-turbulence wind tunnel at the Portuguese National Laboratory for Civil Engineering (LNEC), testing a smooth baseline cylinder and three spaced-strake configurations with gaps correspondent to 20, 40 and 60% of the strake height. The objectives of this investigation are:

1. To determine whether spaced strakes can maintain VIV suppression without significantly increasing drag.
2. To analyse the influence of the gap on wake organisation and vortex-shedding coherence through surface-pressure measurements.
3. To compare the aerodynamic performance of different gap configurations and identify a potential optimal spacing.
4. To evaluate the feasibility of the spaced-strake concept as a practical alternative to conventional attached strakes.

2- BACKGROUND

Flow over a circular cylinder is primarily governed by the Reynolds number, which controls the transition from laminar separation to periodic vortex shedding and turbulent wake development. In the subcritical regime ($Re<10^5$), boundary layers separate before transition, producing periodic shedding and strong pressure fluctuations that can induce vortex-induced vibrations (VIV) [2].

Among passive control strategies, helical strakes are highly effective in suppressing VIV by disrupting spanwise coherence [2,3]. Typically consisting of three fins of height h≈0.1D, they promote three-dimensional separation and inhibit organized Kármán vortices, significantly reducing fluctuating lift [4].

This benefit comes at the cost of increased drag: attached strakes raise C_D from ~1.0–1.2 to 1.35–1.6 (≈15–30% increase) [3,5,6], while reducing lift fluctuations by ~70% [4,7].

However, fixed separation at the fin edges sustains a low base pressure and high drag. Introducing a gap between the strake and cylinder may weaken this effect, allowing partial pressure recovery while maintaining wake decoherence. The present study experimentally investigates this spaced-strake concept in the subcritical regime.

3- IMPLEMENTATION

3.1. Model Design and Fabrication

The experimental models were based on a reference cylinder previously used at LNEC [8]. Four PVC cylinders were assembled: one smooth baseline and three with helical strakes. All had D = 63 mm, thickness 2 mm, and length 586 mm. All models were instrumented with an optimized pressure-tap grid and split longitudinally for internal access. The baseline included a control ring 25 mm below the top (30° spacing).

Strakes had h = 5 mm ($h/D \approx 0.08$), thickness 0.5 mm, and length 216 mm (0.75 turns), giving $p/D \approx 4.6$, starting 50 mm below the top. Gaps of 1, 2, and 3 mm (0.2h, 0.4h, 0.6h) from the surface named the tested configurations: **0.2h-Gap**, **0.4h-Gap**, **0.6h-Gap**.

Strakes were fabricated via resin-based SLS using an ELEGOO Saturn 4 Ultra. Spacing was ensured using 3 mm tube connectors bonded with cyanoacrylate. Three strakes were positioned at 0°, 90° counterclockwise (CCW), and 120° clockwise (CW).

An internal support (30 mm aluminium tube, wooden rings, and 3D-printed connector) ensured alignment and routing of pressure tubing. One connector was printed in ASA at Instituto Superior Técnico, the others in PLA at LNEC. The cylinder halves were sealed with duct tape to prevent leakage (Figure 1).

Fig. 1 | 0.2h-Gap model under testing – LNEC wind tunnel.

3.2. Experimental Facilities

The experiments were conducted in the low-speed closed-circuit wind tunnel at LNEC. The test section (3.0 × 1.2 × 1.0 m) operates up to 45 m/s with turbulence intensity <1%, ensuring subcritical conditions [9]. Velocity was measured using a 5 mm Pitot–Prandtl tube and a BETZ micromanometer (±0.5 Pa), with traceable calibration.

Forces were measured with a six-component balance (developed prior at IST) at 80 Hz for 70 s, calibrated via weighted loads [10], using a relative strain approach referenced to the non-loaded condition (cylinder installed in the tunnel).

Pressures were acquired via taps distributed in the wake region: at z = 13, 15, 17 cm (120°–240°) and z = 19 cm (150°–210°), connected to a PSI PressureSystems 64-channel scanner, sampled at 100 Hz for 60 s.

The model was mounted on a rigid internal support (aluminium spine and wooden rings), ensuring alignment with the flow and minimizing leakage and external disturbances.

4- EXPERIMENTAL VALIDATION

As an introductory remark, the experimental objectives are recalled to frame the validation. The baseline configuration was tested to verify the experimental procedure and measurement accuracy. The spaced–strake models were then assessed to quantify the aerodynamic effect of the gap and its influence on vortex-shedding suppression. Although a conventional attached-strake configuration was not tested, literature data were used for comparison, enabling evaluation against established solutions. Free-stream temperature and air properties were monitored throughout to ensure accurate flow characterization and data consistency.

4.1. Experimental Matrix

For each configuration, seven free-stream velocities (4–30 m/s) were tested, corresponding to $1.5 \times 10^4 \leq Re \leq 1.1 \times 10^5$, within the subcritical regime. Each case (configuration × velocity) was repeated six times to ensure repeatability and statistical reliability.

Free-stream temperature was recorded at the start and end of each run and averaged to compute air density (Ideal Gas Law) and viscosity (Sutherland's law). Mean temperatures ranged from 36.6 °C to 43.3 °C, yielding <3% variation in air properties; within each test, fluctuations remained below 0.7 °C, ensuring nearly constant Reynolds number.

A consistent protocol—model installation, flow stabilization, data acquisition, and signal validation—was applied to all tests to ensure comparability.

4.2. Analysis Methods

The same processing procedure was applied to baseline and spaced-strake models data. Force balance strains were mapped to forces using the selected calibration and nondimensionalized with the smooth cylinder reference area. Signals were divided into 60 non-overlapping 1-second blocks to reduce autocorrelation; the normality of block means was verified via QQ-plots, and all confidence intervals were computed using Student's t distribution. Repetition means were screened for outliers before aggregation. In this way, the mean drag coefficient within each repetition was computed using the following equations:

$$C_D = \frac{1}{N}\sum_{i=1}^{N} C_{D,i} \qquad SE = \frac{s_N}{\sqrt{N}} \qquad C_D \pm t_{0.975,\nu} SE \tag{1}$$

For the RMS fluctuating lift, knowing that $C_L'(t) = C_L(t) - \bar{c}_L$, it is possible to obtain

$$C'_L, rms^{(j)} = \sqrt{\frac{1}{L}\sum_{l=1}^{L}(C'_L(t_l))^2} \tag{2}$$

Pressure taps provided $C_P(\theta, t)$ and C_{Pb}; the Fast Fourier Transform (FFT) of Cp was used to determine the Strouhal number, St, whenever the sampling frequency allowed. Figure 2 presents the scattered results obtained for baseline configuration at 20 m/s for the drag coefficient, represented in the form of boxplots.

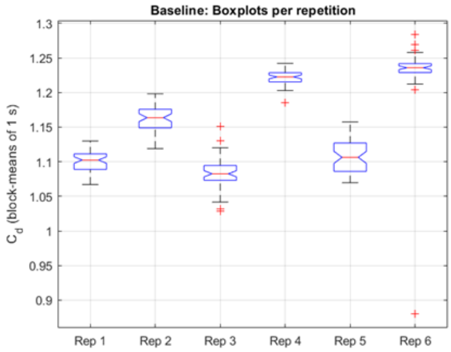

Fig. 2 | Boxplots of mean drag coefficient values at Re = 7.5 × $\mathbf{10^4}$ for baseline configuration.

This velocity corresponds to one of the lowest tested Reynolds numbers and therefore exhibits the largest relative measurement uncertainty. The larger dispersion observed in this case highlights the limitations of the force balance when operating at low signal levels. Accordingly, the results corresponding to Re = 7.5×$\mathbf{10^4}$–1.1×$\mathbf{10^5}$ were analysed, with the case at Re = 7.5 × $\mathbf{10^4}$ (20 m/s) interpreted mainly as indicative of the general trend rather than as an accurate absolute measurement, due to the higher relative uncertainty of the balance at low force levels.

4.3. Baseline Results

The results for both the mean drag and lift coefficients are shown in Figure 3. A representative 2-second segment is displayed to illustrate the oscillatory nature of the aerodynamic forces. The drag coefficient fluctuates around a mean value of approximately C_D = 1.13, while the lift coefficient oscillates symmetrically around zero, as expected for a smooth circular cylinder under nominally uniform crossflow. The time-averaged drag and fluctuating lift coefficients obtained for the smooth baseline cylinder are summarized in Table 1. The results demonstrate excellent repeatability and are consistent with the well-established behaviour of smooth circular cylinders in the subcritical regime.

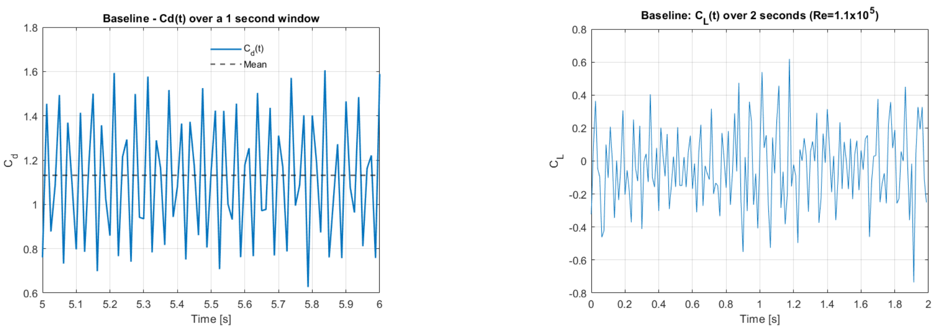

(a) (b)

Fig. 3 | Mean drag (a) and lift (b) coefficients signal over 2-second window for baseline configuration at Re=1.1× $\mathbf{10^5}$.

Table 1 | Mean drag and RMS fluctuating lift coefficients obtained for smooth cylinder, at different Reynolds.

Reynolds	C_D (95% CI, n=6)	$C'_{L,rms}$ ($\pm\sigma$)
7.44×10^4	1.15 ± 0.07	0.36 ± 0.07
9.41×10^4	1.15 ± 0.09	0.24 ± 0.05
1.12×10^5	1.13 ± 0.03	0.23 ± 0.02

The mean drag coefficient remains nearly constant over Re=$7.4\times10^4-1.1\times10^5$, with $C_D\approx1.15$, in agreement with classical data (C_D=1.0−1.2 for Re~10^5[11]). A slight decrease with increasing Reynolds number is also observed, as expected.

The fluctuating lift decreases from $C_{L,rms}$=0.36 at Re=7.4×10^4 to 0.23 at Re=1.1×10^5. The lower-Re value is slightly above typical ranges (0.20−0.30 [11]) but remains within uncertainty, likely due to reduced signal-to-noise at low loads. At higher Reynolds numbers, results align well with reference data, confirming calibration and methodology.

Surface pressure measurements show excellent repeatability and agreement with canonical Cp(θ) distributions. The base pressure (Figure 4(a)) remains nearly constant, $C_{Pb}\approx$−1.05±0.03, consistent with literature [11]. FFT analysis yields shedding peaks at St≈0.17−0.18 (Figure 4(b)), confirming accurate capture of vortex shedding.

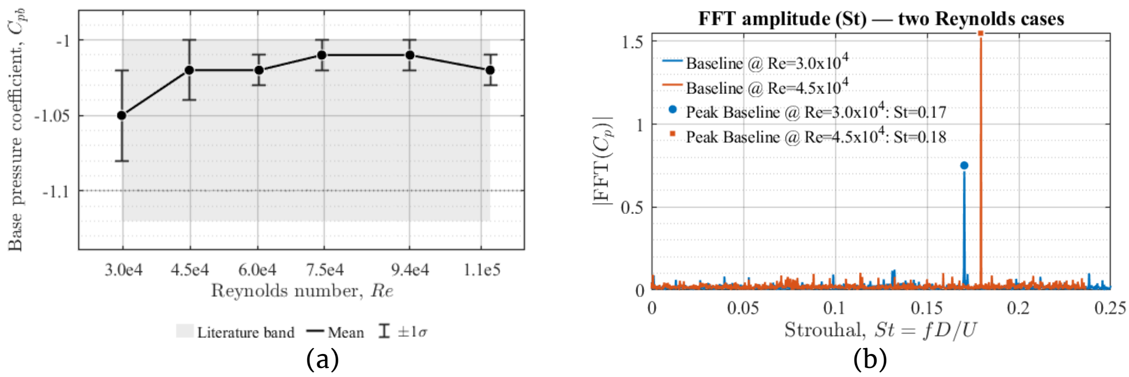

Fig. 4 | Base pressure coefficient (a) and frequency analysis (b) - Baseline pressure-field validation.

5- SPACED STRAKES RESULTS

Tables 2−4 summarize C_D, $C_{L,rms}$, and C_{Pb} for the 0.2h-, 0.4h-, and 0.6h-Gap configurations at 20−30 m/s (7.4×10^4 < Re < 1.1×10^5), benchmarked against the smooth baseline. Base pressure was taken at z/D = 2.4 to represent global wake behaviour without direct strake interference. Baseline values ($C_{Pb}\approx$ −0.68) are consistent with canonical subcritical data.

Table 2 | Mean drag, RMS fluctuating lift and base pressure coefficients obtained for 0.2h-Gap, at different Reynolds.

Reynolds	C_D ($\pm\sigma$)	$C'_{L,rms}$ ($\pm\sigma$)	C_{pb}
7.44×10^4	1.41 ± 0.15	0.25 ± 0.04	−0.746
9.41×10^4	1.30 ± 0.16	0.15 ± 0.02	−0.748
1.12×10^5	1.22 ± 0.05	0.13 ± 0.01	−0.736

The 0.2h-Gap configuration shows the highest drag penalty, approaching attached-strake behaviour. Despite higher uncertainty at low velocity, C_D remains above both the baseline and wider gaps. The more negative C_{Pb} indicates a stronger base-pressure deficit and wider wake. The values of $C_{L,rms}$ are reduced relative to the smooth cylinder, confirming that vortex-shedding disruption remains active.

Table 3 | Mean drag, RMS fluctuating lift and base pressure coefficients obtained for 0.4h-Gap, at different Reynolds.

Reynolds	C_D $(\pm\sigma)$	$C'_{L,rms}$ $(\pm\sigma)$	C_{pb}
7.44×10^4	1.37 ± 0.07	0.18 ± 0.07	-0.728
9.41×10^4	1.20 ± 0.04	0.13 ± 0.01	-0.718
1.12×10^5	1.14 ± 0.01	0.09 ± 0.01	-0.696

At 0.4h, drag decreases consistently, approaching baseline values at higher Reynolds numbers. This is accompanied by a less negative C_{Pb}, indicating partial wake recovery. The values of $C_{L,rms}$ remain reduced relative to the smooth case, showing that vortex-shedding suppression is maintained.

The 0.6h-Gap configuration provides the most favourable drag behaviour. At Re ≥ 9.4×10^4, C_D approaches smooth-cylinder values with consistent trends and reduced uncertainty. The base pressure is the least negative among straked cases, confirming reduced wake deficit. The values of $C_{L,rms}$ remain consistently low, indicating that the attenuation of unsteady lift is preserved.

Table 4 | Mean drag, RMS fluctuating lift and base pressure coefficients obtained for 0.6h-Gap, at different Reynolds.

Reynolds	C_D $(\pm\sigma)$	$C'_{L,rms}$ $(\pm\sigma)$	C_{pb}
7.44×10^4	1.35 ± 0.13	0.11 ± 0.03	-0.704
9.41×10^4	1.18 ± 0.08	0.12 ± 0.01	-0.701
1.12×10^5	1.13 ± 0.05	0.07 ± 0.01	-0.684

Table 5 quantifies the progressive reduction in drag penalty with increasing gap, approaching smooth-cylinder values and outperforming classical attached strakes. Table 6 shows that all configurations maintain a substantial reduction in fluctuating lift (≈50%), confirming that vortex-shedding disruption persists across all tested gaps.

PSD analysis (Welch method) shows that for Re ≲ 4.5×10^4, straked configurations exhibit broadband spectra without a dominant peak at St ≈ 0.2 (Figure 5), indicating loss of spanwise coherence. This behaviour is consistent with the observed reduction in $\boldsymbol{C_{L,rms}}$ and is expected to persist at higher Reynolds numbers. The PSD was computed using Welch's method (Hann windows, 50% overlap), with reliable peak detection limited to $U_\infty \leq 12$ m/s due to the 100 Hz sampling frequency; within this range, the absence of a distinct spectral peak confirms the disruption of coherent vortex shedding.

Table 5 | Percentage increase in the mean drag coefficient, C_D, relative to baseline for different Reynolds.

Configuration\Reynolds	7.44×10^4	9.41×10^4	1.12×10^5
Attached		$\sim 17 - 26\%$	
0.2h-Gap	~27%	~19%	~17%
0.4h-Gap	~13%	~4%	~3%
0.6h-Gap	~9%	~2%	~1%

Table 6 | Percentage reduction in RMS fluctuating lift coefficient, $C'_{L,rms}$, compared to Baseline.

Configuration\Reynolds	7.44×10^4	9.41×10^4	1.12×10^5
Attached		~ 50 − 70%	
0.2h-Gap	~31%	~49%	~70%
0.4h-Gap	~37%	~42%	~51%
0.6h-Gap	~43%	~59%	~70%

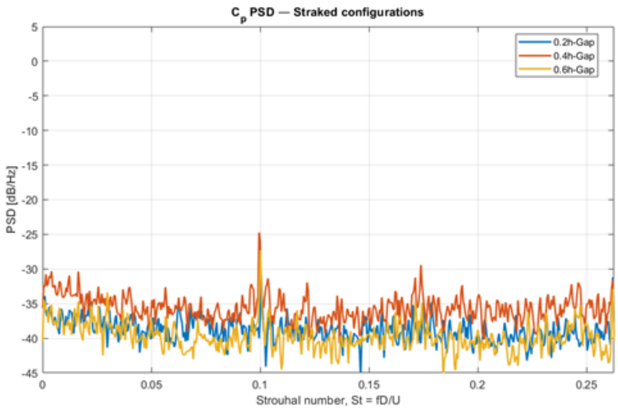

Fig. 5 | PSD of the C_P(t) signal using Welch's method, at Re=4.5×10^4.

5.1. Performance of Optimal Spaced Configuration

The baseline pressure distribution confirms the expected subcritical behaviour of a smooth circular cylinder. As shown in Figure 6, the mean field is spanwise uniform, with horizontal isolines and a strong suction region on the rear surface, indicating coherent, two-dimensional vortex shedding, consistent with literature [2,11].

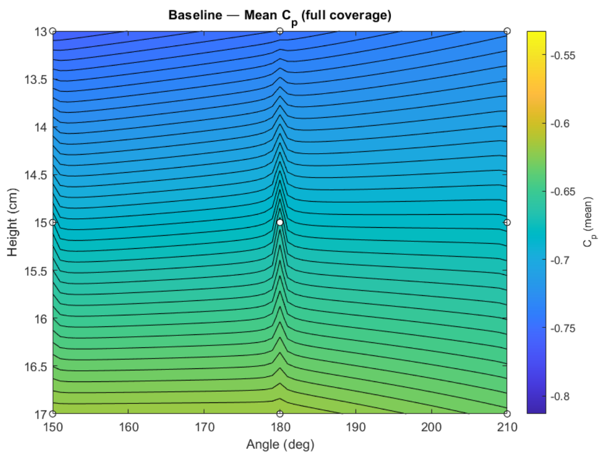

Fig. 6 | Mean pressure coefficient map, C_P, of baseline configuration at Re = 1.1 × 105.

In contrast, the straked configurations (Figure 7) show a clear wake modification. Helical ridges appear as regions of higher pressure (yellow tone) along the strake trajectory, marking the interaction between separated shear layers and bleed flow through the gap. This flow introduces higher-pressure fluid into the wake, reducing suction peaks and weakening vortex coherence.

As spacing increases from 0.2h to 0.6h, this effect becomes more pronounced. Larger gaps enhance momentum exchange, energizing shear layers, narrowing the wake, and producing a less negative pressure field. Since a narrower wake is associated with higher base pressure and lower drag [11,12], this explains the improved aerodynamic behaviour.

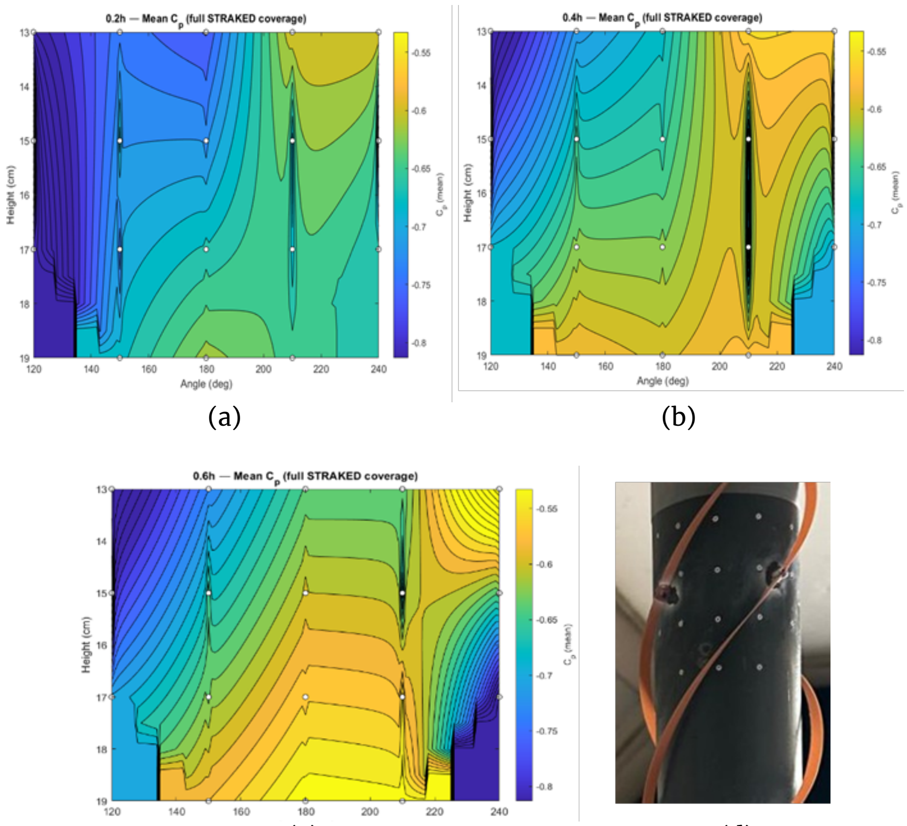

(a) (b)

(c) (d)

Fig. 7 | Mean pressure coefficient map, C_P, of all straked configurations at Re = 1.1×105.

The 0.6h-Gap case shows the most favourable local feature, with reduced suction and higher pressure along the helical trajectory (Figure 7.d). This confirms that controlled spacing disrupts spanwise coherence while promoting pressure recovery, consistent with mechanisms reported in [13].

6- CONCLUSIONS

The application of spaced helical strakes incorporating a finite gap in circular cylinders was experimentally investigated aiming to retain vortex-induced vibration (VIV) suppression while reducing drag penalties. A smooth baseline and three spaced configurations (0.2h, 0.4h, 0.6h) were tested in the LNEC wind tunnel for $10^4 < Re < 10^5$. Baseline validation showed good agreement with classical drag, lift, and Strouhal values.

Introducing a gap significantly reduced drag penalties without compromising VIV suppression. The 0.6h-Gap performed best, with drag increases of only 1–9% relative to the smooth cylinder—well below the 17–26% typical of attached strakes—while reducing fluctuating lift by 43–70%. Pressure distributions indicated enhanced momentum exchange, reduced wake width, and partial pressure recovery, explaining the improved performance.

These results show that spaced helical strakes offer an effective compromise between aerodynamic efficiency and vibration suppression, representing a promising alternative to conventional designs.

ACKNOWLEDGMENTS

The authors gratefully acknowledge the staff of IST and LNEC for their invaluable support and for providing access to the facilities used throughout this work. The authors also wish to express their sincere appreciation to Prof. Mário Vaz for his exemplary organization of APAET 2026, as well as to APAET for the opportunity to publish this work in its prestigious journal.

REFERENCES

1. Choi, H. et al. Control of flow over a bluff body. Annual Review of Fluid Mechanics, 2008, DOI: 10.1146/annurev.fluid.39.050905.110149.
2. Blevins, R.D. et al. Flow-Induced Vibrations. Van Nostrand Reinhold, 1990.
3. Zdravkovich, M.M. et al. Review and classification of various aerodynamic and hydrodynamic means for suppressing vortex shedding. Journal of Wind Engineering and Industrial Aerodynamics, 1981, DOI: 10.1016/0167-6105(81)90036-2
4. Zhou, T. et al. On the study of vortex-induced vibration of a cylinder with helical strakes. Journal of Fluids and Structures, 2011, DOI: 10.1016/j.jfluidstructs.2011.06.005.
5. Branković, M. et al. Measurements of transverse forces on circular cylinders undergoing vortex-induced vibration. Journal of Fluids and Structures, 2006, DOI: 10.1016/j.jfluidstructs.2006.04.006.
6. Cowdrey, C.F. et al. Drag measurements at high Reynolds numbers of a circular cylinder fitted with three helical strakes. Aero Report 384, National Physical Laboratory, 1959.
7. Sui, Y. et al. Vortex-induced vibration suppression for a large mass-damping cylinder attached with helical strakes. Journal of Fluids and Structures, 2016, DOI: 10.1016/j.jfluidstructs.2016.01.006.
8. Borges, A.R.J. et al. Ensaio em túnel aerodinâmico de uma torre de antena de televisão. Relatório Técnico LNEC, 1970.

9. Borges, A.R.J. et al. O túnel aerodinâmico do laboratório nacional de engenharia civil: Parte I — descrição geral. Memória LNEC 319, 1968.
10. Pacheco, J.R.M. et al. Wind tunnel testing of a complete formula student vehicle. Master's Thesis, Instituto Superior Técnico, 2022.
11. Zdravkovich, M.M. et al. Flow Around Circular Cylinders. Oxford University Press, 1997.
12. Roshko, A. et al. On the wake and drag of bluff bodies. Journal of the Aeronautical Sciences, 1955, DOI: 10.2514/8.3284.
13. Sevilla, A. et al. Vortex shedding in high Reynolds number axisymmetric bluff-body wakes: Local linear instability and global bleed control. Physics of Fluids, 2004, DOI: 10.1063/1.1777561.